Hydrogen Evolution Reaction

DOI: 10.1002/ange.201311111

Cobalt-Embedded Nitrogen-Rich Carbon Nanotubes Efficiently Catalyze Hydrogen Evolution Reaction at All pH Values**

*Xiaoxin Zou, Xiaoxi Huang, Anandarup Goswami, Rafael Silva, Bhaskar R. Sathe, Eliška Mikmeková, and Tewodros Asefa**

Abstract: *Despite being technically possible, splitting water to generate hydrogen is still practically unfeasible due mainly to the lack of sustainable and efficient catalysts for the half reactions involved. Herein we report the synthesis of cobalt-embedded nitrogen-rich carbon nanotubes (NRCNTs) that 1) can efficiently electrocatalyze the hydrogen evolution reaction (HER) with activities close to that of Pt and 2) function well under acidic, neutral or basic media alike, allowing them to be coupled with the best available oxygen-evolving catalysts—which also play crucial roles in the overall water-splitting reaction. The materials are synthesized by a simple, easily scalable synthetic route involving thermal treatment of Co^{2+}-embedded graphitic carbon nitride derived from inexpensive starting materials (dicyandiamide and $CoCl_2$). The materials' efficient catalytic activity is mainly attributed to their nitrogen dopants and concomitant structural defects.*

As being the cleanest of all fuels, hydrogen has long been expected to play a pivotal role in our energy landscapes by mitigating, if not completely eliminating, our reliance on fossil fuels.[1] However, this hype has so far been elusive, mainly because: 1) molecular hydrogen does not exist naturally on earth, 2) the production of molecular hydrogen from water—the most abundant and renewable hydrogen source—by the water-splitting reaction is inherently quite difficult, and 3) there is a lack of sustainable catalysts composed of inexpensive and earth-abundant elements that can efficiently catalyze the half reactions involved in the water-splitting reaction.[2]

The water-splitting reaction can be viewed as a combination of two half reactions: the hydrogen evolution reaction (HER) and the oxygen evolution reaction (OER).[2] To conduct electrochemical water splitting, voltages above the thermodynamic potential values corresponding to the intrinsic activation barriers present in both half reactions (also known as overpotential, η) must be applied. Hence, reduction of both overpotentials using HER or OER catalysts, respectively, is essential to make the water-splitting reaction less energy-intensive. Unfortunately, it is difficult to find suitable HER and OER catalysts that can work well in the same pH range to be coupled together and make the overall water-splitting reaction more energy-efficient. Whereas almost all the best OER catalysts (especially those synthesized from earth-abundant elements) work well only in neutral or basic media,[2–5] most of the recently developed HER catalysts function well only in acidic media (except for very few that can work in neutral and basic media, see Tables S1–S3 in the Supporting Information).[6–25] Finding competent HER catalysts that can operate in a wide pH range (and hence have the potential to work well with the best OER catalysts regardless of pH) may address one of the major issues currently plaguing the water-splitting reaction, especially when OER catalysts that can work in a wide pH range are relatively rare.

Although Pt-based catalysts are known to efficiently catalyze HER almost irrespective of pH, their widespread use has been limited by their low earth-abundance and high cost. Hence, the development of HER catalysts that are composed of inexpensive and earth-abundant elements and can catalyze HER has been one of the main targets in renewable energy research in recent years. Some of these efforts have already led to some notable noble metal-free or transition metal complex-based HER catalysts (e.g., Ni/Co macrocycles and Ni diphosphine complexes);[26] however, most of such homogenous catalysts were shown to only work in organic media. This problem has been circumvented for some of these catalysts by supporting them on HER-inactive carbon nanotubes (CNTs), which yielded heterogeneous catalysts that catalyze HER in aqueous acidic solutions.[27] Recently, some solid-state non-Pt-based systems have also emerged as efficient HER catalysts under various conditions, which include 1) metal sulfides, nitrides, borides and phosphides (e.g., MoS_2 and Ni-Mo-N) in acidic solution[6–23] and 2) metal, metal alloys and metal oxides/sulfides (e.g., Ni, Ni–Mo alloy, CoO_x: PO_4 and Co-S) in neutral or alkaline media (Tables S1–S3).[23–25,28]

[*] Dr. X. Zou, X. Huang, Dr. A. Goswami, Dr. R. Silva, Dr. B. R. Sathe, Prof. T. Asefa
Department of Chemistry and Chemical Biology
Rutgers, The State University of New Jersey
610 Taylor Road, Piscataway, NJ 08854 (USA)
E-mail: tasefa@rci.rutgers.edu
Dr. X. Zou, Dr. A. Goswami, Dr. B. R. Sathe, Prof. T. Asefa
Department of Chemical and Biochemical Engineering
Rutgers, The State University of New Jersey
98 Brett Road, Piscataway, NJ 08854 (USA)
Dr. X. Zou
State Key Laboratory of Inorganic Synthesis & Preparative Chemistry, College of Chemistry, Jilin University
2699 Qianjin Street, Changchun 130012 (China)
E. Mikmeková
Institute of Scientific Instruments of the ASCR, v.v.i.
Kralovopolska 147, Brno 612 64 (Czech Republic)

[**] T.A. gratefully acknowledges the financial assistance of the National Science Foundation (DMR-0968937, CBET-1134289, NSF-ACIF, and NSF Special Creativity grant).

Supporting information for this article is available on the WWW under http://dx.doi.org/10.1002/anie.201311111.

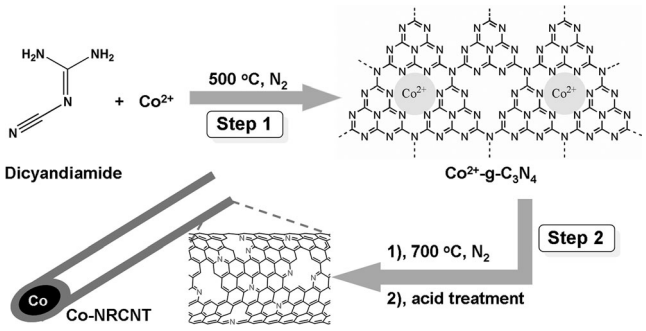

Figure 1. Synthesis of Co-NRCNTs: Step 1: thermal treatment at 500 °C in N_2 atmosphere of a mixture of dicyandiamide and $CoCl_2 \cdot 6H_2O$ to form Co^{2+}-g-C_3N_4. Step 2: additional thermal treatment at 700 °C in N_2 atmosphere of the Co^{2+}-g-C_3N_4, followed by acid treatment of the resulting material to etch away any accessible cobalt species on it.

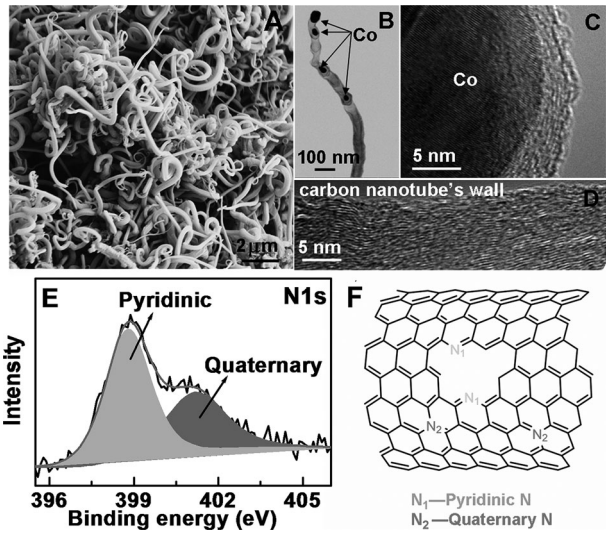

Figure 2. A) SEM image, B–D) STEM images, and E) N1s XPS spectrum of Co-NRCNTs. In the XPS spectrum, the raw curve (black) is peak-fitted into two curves (indicated by light gray and gray shaded areas) that correspond to two different types of N species (pyridinic and quaternary), and the sum of the two peak-fitted curves is shown with the gray curve. F) Representation of the two types of N dopants present in the Co-NRCNTs based on XPS results.

Herein we report the synthesis of cobalt-embedded nitrogen-rich CNTs (Co-NRCNTs) (Figure 1) that can serve as highly active electrocatalyst for HER under acidic, neutral or basic media alike to be easily coupled with the best OER catalysts available. Despite recent studies on the electrocatalytic activities of N-doped and/or metal-containing CNTs for OER and ORR[29] and the use of HER-inactive CNTs as support material for HER-active transition metal complexes,[27] this is the first time a CNT-based material is reported to catalyze HER on its own.

As illustrated in Figure 1, the synthesis of Co-NRCNTs is achieved by simple thermal treatment of Co^{2+}-functionalized graphitic carbon nitride (Co^{2+}-g-C_3N_4) at 700 °C in N_2 atmosphere, followed by acid treatment of the resulting material with 0.5 M H_2SO_4 for 24 h to remove any accessible cobalt species present on it. The precursor Co^{2+}-g-C_3N_4 is prepared in one step through self-assembly of inexpensive starting materials (dicyandiamide and $CoCl_2 \cdot 6H_2O$, Step 1) (for detailed characterization results of the precursor material, please see our previous report[30]).

Scanning electron microscopy (SEM) image (Figure 2A) and scanning transmission electron microscopy (STEM) images (Figure 2B and S1) show that the Co-NRCNTs are several μm long and 20–100 nm thick multi-walled CNTs (MWCNTs). The STEM images (Figure 2B and C) further indicate the presence of some carbon-encapsulated Co nanoparticles, especially at one of the two endpoints of the Co-NRCNTs. These carbon-encased Co nanoparticles are quite inaccessible as they remain embedded within the nanotubes even after treatment of the Co-NRCNTs with acidic solution. Furthermore, the STEM images in Figure 2C and D reveal that the CNTs, including the carbon shells around the Co nanoparticles, are crystalline. The presence of metallic cobalt and crystalline carbon in Co-NRCNTs is confirmed by powder X-ray diffraction (XRD) and X-ray photoelectron spectroscopy (XPS) (Figure S2 and S3). Based on thermogravimetric analysis (TGA), the Co/C atomic ratio and the wt.% of Co in the Co-NRCNTs are found to be 1.5:100 and 6.9%, respectively. The N1s XPS spectrum of Co-NRCNTs (Figure 2E) further shows the presence of two types of nitrogen species, which can be attributed to pyridinic (N1s in Figure 2F) and quaternary (N2s in Figure 2F) nitrogen atoms, respectively. Further quantitative analysis of the XPS results reveals that the atomic ratios of N/C [or (N1 + N2)/C], N1/C and N2/C in the Co-NRCNTs are 5.2:100, 3.7:100, and 1.5:100, respectively.

It is worth noting here that when pure g-C_3N_4 instead of Co^{2+}-g-C_3N_4 was used as precursor under otherwise identical synthetic conditions, no carbon material was obtained as product. In other words, in absence of Co^{2+} ions in its structure, g-C_3N_4 did not lead to carbon upon pyrolysis. Since Co nanoparticles are known to catalyze the formation of CNTs from a variety of organic precursors,[31] the growth of Co-NRCNTs is likely to occur via some decomposition intermediates of g-C_3N_4[32] aided by Co nanoparticles formed in situ from the Co^{2+} ions in Co^{2+}-g-C_3N_4 during pyrolysis.

The micro-Raman spectrum of Co-NRCNTs (Figure S4) displays the characteristic D and G bands of CNTs. The D band, which originates from hybridized vibrational mode associated with the edges of CNTs, is often referred to as the disorder or defect band whereas the G band is related to the tangential oscillations and vibrations of all the sp^2 carbon atoms in the CNTs. Therefore, the intensity ratio between D and G bands (I_D/I_G) is often used as a measure of defect density in CNTs. In the case of Co-NRCNTs, I_D/I_G is found to be 0.66; this suggests the presence of significant structural defects or microstructural rearrangement of the atoms within Co-NRCNTs, presumably stemming from the presence of N dopants and concomitant absence of C atoms in the structure of Co-NRCNTs.

The electrocatalytic activity of Co-NRCNTs toward HER at various pH values was evaluated using a typical three-electrode system, which consists of a glassy carbon electrode

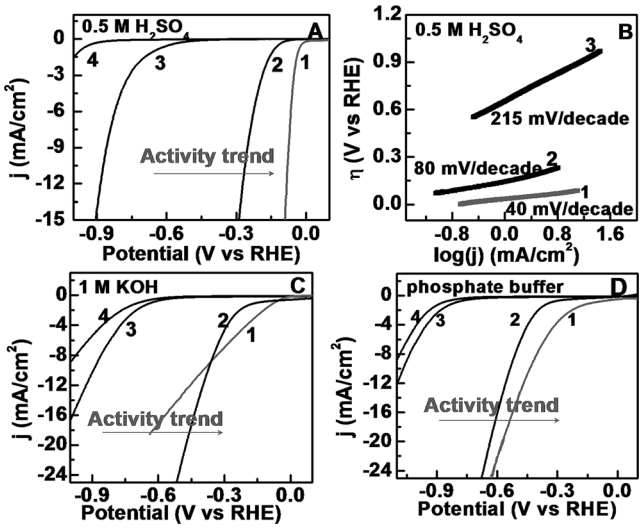

Figure 3. A) Linear sweep voltammetry (LSV) curves in 0.5 M H_2SO_4 (pH 0), B) the corresponding Tafel plots in H_2SO_4 solution, and LSV curves in C) 1 M KOH (pH 14) and D) phosphate buffer (pH 7) solutions. Sample labels are: **1**, 1 wt.% Pt/C; **2**, Co-NRCNTs; **3**, MWCNTs; and **4**, no catalyst. The sample loading on the GCE is 0.28 mg cm^{-2} in all the cases, and the obtained current densities are all normalized with the surface area of the GCE.

(GCE) modified with Co-NRCNTs as the working electrode (see Supporting Information). For comparison, the electrocatalytic activity of commercially available nitrogen-free MWCNTs and 1 wt.% Pt nanoparticles on activated carbon (Pt/C) was also measured.

Our first electrochemical experiment involved measurement of the electrocatalytic activity of Co-NRCNTs in acidic media (0.5 M H_2SO_4). As shown in Figure 3A, the Co-NRCNTs exhibit a small onset potential of −0.05 V toward HER (curve 1), with a cathodic current that rises rapidly as more negative potential is applied. The result reveals that the onset potential of Co-NRCNTs is very close to the thermodynamic potential of HER (i.e., 0 V) and is much better than that of MWCNTs (−0.44 V, curve 3). Accordingly, Co-NRCNTs give a smaller Tafel slope (69 mV/decade) and a higher exchange current density (1×10^{-2} mA cm^{-2}) compared with MWCNTs (Tafel slope = 215 mV/decade and exchange current density = 1×10^{-3} mA cm^{-2}) (Figure 3B). Additionally, Co-NRCNTs afford current densities of 1 mA cm^{-2} and 10 mA cm^{-2} at $\eta = 0.14$ V and 0.26 V, respectively. These findings demonstrate Co-NRCNTs' superior electrocatalytic activity toward HER compared with MWCNTs. The results also make Co-NRCNTs among the most active noble metal-free heterogeneous HER catalysts for acidic media (see Table S1). For example, CNT-supported diimine-dioxime cobalt complexes show lower current density of 1 mA cm^{-2} at $\eta = 0.59$ V,[27a] and Ni–Mo nitride nanosheets ($NiMoN_x$) require an overpotential of 0.15 V for HER.[21] Moreover, some Mo-based compounds including sulfides, carbides and borides give a current density of 10 mA cm^{-2} at $\eta = 0.15$–0.3 V,[10–23] and nanostructured Ni_2P requires an overpotential of 0.1 V.[6]

Next, the electrocatalytic activity of Co-NRCNTs for HER in basic media was studied (1 M KOH, pH 14, Figure 3C). As shown in Figure 3C, whereas the catalytic activity of MWCNTs is almost similar to that of the blank reaction, Co-NRCNTs exhibit very good electrocatalytic activity for HER in basic media as well. When compared with Pt/C's onset potential in basic media, the onset potential of Co-NRCNTs is only marginally lower, by −0.05 to −0.1 V under the same conditions. Interestingly, at slightly higher applied potentials than their onset potential (< −0.5 V vs. RHE), Co-NRCNTs actually give higher current density, which means greater electrocatalytic activity, than Pt/C does. Moreover, the catalytic activity of Co-NRCNTs is also comparable to some of the best non-noble metal HER catalysts for basic media (e.g., Ni)[23] (Table S2).

Performing electrocatalytic reactions under neutral media is generally preferred as under this condition reactions are more benign and most electrocatalysts are stable against corrosion, oxidation, etc. Thus, after investigating the catalytic activity of Co-NRCNTs in both acidic and basic media, we focused our attention to Co-NRCNTs' catalytic activity in neutral media, despite HER's inherently slow kinetics under this condition.[23] Not surprisingly, Co-NRCNTs' electrocatalytic activity at pH 7 is relatively lower than the ones at pH 0 or pH 14. For instance, while Co-NRCNTs give a current density of 1 mA cm^{-2} at overpotentials of 0.14 V and 0.16 V at pH 0 and 14, respectively, Co-NRCNTs exhibit the same current density at a much higher overpotential of 0.33 V at pH 7. Nevertheless, Co-NRCNTs' catalytic performance is still much better than MWCNTs' (Figure 3D) and is, in fact, very close to Pt/C's. In addition, Co-NRCNTs' catalytic activity in neutral media is as good as that of metallic cobalt@cobalt-oxo/hydroxo phosphate[24]—one of the best noble metal-free HER catalysts reported for neutral media (Table S3).

To assess the stability of Co-NRCNTs in HER, the potentiostatic hydrogen evolution reaction in the presence of Co-NRCNTs was carried out for longer time periods under acidic (pH 0), neutral (pH 7), or basic media (pH 14). As shown in Figure S5–S7, the Co-NRCNTs retained their electrocatalytic activity, giving a constant current density of ca. 1 mA cm^{-2} for 8.5–10 h in each case. Moreover, Co-NRCNTs gave nearly 100% Faradaic yield during hydrogen evolution in all the three cases (Figure S8). These results indicate Co-NRCNTs' great stability in HER under a wide pH range.

Additional studies were conducted to get some insights into the origin of the superior catalytic activity of Co-NRCNTs as well as their structure–catalytic activity relationships. This primarily included the synthesis of materials by pyrolysis of the Co-NRCNTs at higher temperatures (800, 900, 1000, 1100, and 1200 °C), followed by investigation of their electrocatalytic properties.Additionally, a series of materials were obtained by pyrolyzing Co^{2+}-g-C_3N_4 at 800, 900, 1000, 1100, and 1200 °C (whose SEM and TEM images are displayed in Figure S9), and their electrocatalytic activities were also studied (Figure S10). As the results are almost the same in both cases, only those involving the former are discussed in detail below.

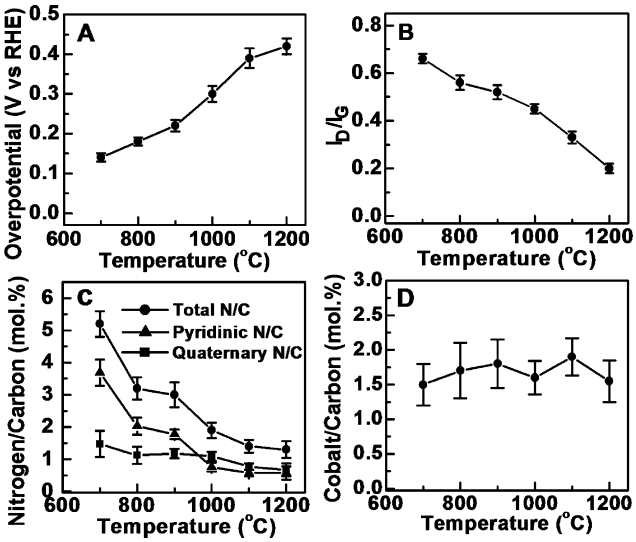

Figure 4. A) Catalytic activity (as measured by the overpotential that the electrocatalyst needs to yield a current density of 1 mA cm^{-2}) in 0.5 M H_2SO_4 (pH 0) as a function of the pyrolysis temperatures employed to synthesize the carbon nanomaterials. (Please note that samples with larger overpotentials have lower electrocatalytic activity.) B) The I_D/I_G value (obtained from FT-Raman spectra), C) the ratios of total N/C, pyridinic N/C and quaternary N/C (obtained from XPS), and D) the ratio of Co/C (obtained from thermogravimetric analysis) as a function of pyrolysis temperatures employed to synthesize the carbon nanomaterials.

Generally, as the pyrolysis temperature is raised from 700 to 1200 °C, the catalytic activity of the materials decreases, as seen from the gradual increase in the overpotentials needed to yield a current density of 1 mA cm^{-2} (Figure 4 A). Moreover, the decrease in catalytic activity appears to correlate well with the decrease in the defect density in the materials; this is evident from the decrease in the I_D/I_G ratio of the materials from 0.66 to 0.20 as the pyrolysis temperature is raised from 700 °C to 1200 °C (Figure 4 B). This result is also in agreement with the poor catalytic activity of MWCNTs, which have a very low I_D/I_G ratio ($\approx$0.2) that corresponds to a very low defect density (Figure S11). In addition, the nitrogen content (both pyridinic and quaternary nitrogen species) in the Co-NRCNTs, as determined by XPS in Figure 4 C, decreases as the pyrolysis temperature increases (Figure 4 B). Interestingly also, the materials showed lower catalytic activity after they were pyrolyzed further at temperatures above 700 °C, despite they still contained almost the same amount and similar type of carbon-encased (metallic) Co nanoparticles (Figure 4 D). Based on the above results, Co-NRCNTs' excellent catalytic performance for HER could be attributed to the N dopants or N dopant-related structural defects.

Given the few recent reports indicating that carbon-encapsulated metal nanoparticles can catalyze electrocatalytic oxygen reduction reaction,[29b,c,33] we had thought that the Co nanoparticles in our case, despite being inaccessible, may still play some roles on the catalytic activity of the materials towards HER. However, since the Co nanoparticles are well encapsulated by carbon and thus not easily removable from the Co-NRCNTs without compromising the structures of the latter, it is difficult to directly determine their possible roles in catalytic process by removing them from the nanotubes. Thus, we resorted to an indirect approach, which involved synthesis of other metal-embedded N-rich CNTs under the same procedure and then investigation of their catalytic activities towards HER. Specifically, we synthesized Ni- and Fe-embedded N-rich CNTs (Ni-NRCNTs and Fe-NRCNTs) by using Ni^{2+} or Fe^{2+} ions, respectively, in place of Co^{2+} ions under otherwise similar synthetic conditions. Results of the electrocatalytic activity of the three materials toward HER (Figure S12) clearly indicates that the materials' catalytic activities increase in the order of Fe-NRCNTs < Ni-NRCNTs < Co-NRCNTs. This result, along with the fact that these three materials have similar CNT structure, nitrogen content, nitrogen type, and metal content, suggests that the metal (or Co) nanoparticles may have contributed to the materials' (or Co-NRCNTs') catalytic activity.

Furthermore, based on this result, coupled with the recent studies on nitrogen-doped and/or metal-containing CNTs for electrocatalysis,[29,33] the following possible cooperative and/or synergistic catalytic effects between the N dopants and carbon-coated Co nanoparticles in Co-NRCNTs can be proposed to account for Co-NRCNTs' enhanced catalytic activity towards HER: 1) Nitrogen atoms are inherently better in interacting with reactants (i.e., protons/water) than carbon atoms due to the presence of lone-pair electrons on the former. Thus, the presence of nitrogen dopants in Co-NRCNTs' would favor both the interaction, and thereby the reactivity, of reactants with the CNTs (or the electrocatalyst). 2) Owing to the relatively higher electronegativity of N compared with that of C, the N dopants in the Co-NRCNTs render higher positive charge density on their adjacent carbon atoms, by virtue of which these carbon atoms could become catalytic active sites.[29d] 3) The presence of metal nanoparticles inside CNTs could result in decreased local work function on the carbon surface owing to facile electron transfer from metal particles to the CNTs.[33] Nevertheless, all these possible scenarios still call for further in-depth mechanistic investigation, especially on an atomic level.

In conclusion, we have reported the synthesis of cobalt-embedded nitrogen-rich CNTs (Co-NRCNTs) that are proven to be highly efficient, non-noble metal-based electrocatalyst for HER. The Co-NRCNTs: 1) contain only earth-abundant elements (C, N and Co); 2) are synthesized with easily scalable and cost-effective synthetic method; 3) operate well as electrocatalyst for HER at low or modest overpotentials; and 4) have the ability to operate over a wide pH range, from pH 0.0 to 14.0. The work can, therefore, encourage further research on the development of other noble-metal-free or metal-free catalysts for renewable energy applications.

Received: December 22, 2013
Revised: February 4, 2013
Published online: March 20, 2014

Keywords: carbon nanotubes · cobalt nanoparticles · electrocatalysis · hydrogen evolution reaction · water splitting

[1] J. A. Turner, *Science* **1999**, *285*, 687.
[2] T. R. Cook, D. K. Dogutan, S. Y. Reece, Y. Surendranath, T. S. Teets, D. G. Nocera, *Chem. Rev.* **2010**, *110*, 6474.
[3] M. W. Kanan, D. G. Nocera, *Science* **2008**, *321*, 1072.
[4] R. D. L. Smith, M. S. Prévot, R. D. Fagan, Z. Zhang, P. A. Sedach, M. K. J. Siu, S. Trudel, C. P. Berlinguette, *Science* **2013**, *340*, 60.
[5] C. L. McCrory, S. Jung, J. C. Peters, T. F. Jaramillo, *J. Am. Chem. Soc.* **2013**, *135*, 16977.
[6] E. J. Popczun, J. R. McKone, C. G. Read, A. J. Biacchi, A. M. Wiltrout, N. S. Lewis, R. E. Schaak, *J. Am. Chem. Soc.* **2013**, *135*, 9267.
[7] B. Hinnemann, P. G. Moses, J. Bonde, K. P. Jørgensen, J. H. Nielsen, S. Horch, I. Chorkendorff, J. K. Nørskov, *J. Am. Chem. Soc.* **2005**, *127*, 5308.
[8] T. F. Jaramillo, K. P. Jørgensen, J. Bonde, J. H. Nielsen, S. Horch, I. Chorkendorff, *Science* **2007**, *317*, 100.
[9] A. B. Laursen, S. Kegnæs, S. Dahl, I. Chorkendorff, *Energy Environ. Sci.* **2012**, *5*, 5577.
[10] D. Merki, H. Vrubel, L. Rovelli, S. Fierroa, X. Hu, *Chem. Sci.* **2012**, *3*, 2515.
[11] D. Merki, S. Fierro, H. Vrubel, X. Hu, *Chem. Sci.* **2011**, *2*, 1262.
[12] Y. Li, H. Wang, L. Xie, Y. Liang, G. Hong, H. Dai, *J. Am. Chem. Soc.* **2011**, *133*, 7296.
[13] M. A. Lukowski, A. S. Daniel, F. Meng, A. Forticaux, L. Li, S. Jin, *J. Am. Chem. Soc.* **2013**, *135*, 10274.
[14] D. Voiry, H. Yamaguchi, J. Li, R. Silva, D. C. B. Alves, T. Fujita, M. Chen, T. Asefa, V. B. Shenoy, G. Eda, M. Chhowalla, *Nat. Mater.* **2013**, *12*, 850.
[15] J. Kibsgaard, Z. Chen, B. N. Reinecke, T. F. Jaramillo, *Nat. Mater.* **2012**, *11*, 963.
[16] J. Xie, H. Zhang, S. Li, R. Wang, X. Sun, M. Zhou, J. Zhou, X. W. Lou, Y. Xie, *Adv. Mater.* **2013**, *25*, 5807.
[17] J. Xie, J. Zhang, S. Li, F. Grote, X. Zhang, H. Zhang, R. Wang, Y. Lei, B. Pan, Y. Xie, *J. Am. Chem. Soc.* **2013**, *135*, 17881.
[18] H. Vrubel, D. Merki, X. Hu, *Energy Environ. Sci.* **2012**, *5*, 6136.
[19] T. F. Jaramillo, J. Bonde, J. Zhang, B.-L. Ooi, K. Andersson, J. Ulstrup, I. Chorkendorff, *J. Phys. Chem. C* **2008**, *112*, 17492.
[20] J. D. Benck, Z. Chen, L. Y. Kuritzky, A. J. Forman, T. F. Jaramillo, *ACS Catal.* **2012**, *2*, 1916.
[21] W.-F. Chen, K. Sasaki, C. Ma, A. I. Frenkel, N. Marinkovic, J. T. Muckerman, Y. Zhu, R. R. Adzic, *Angew. Chem.* **2012**, *124*, 6235; *Angew. Chem. Int. Ed.* **2012**, *51*, 6131.
[22] B. Cao, G. M. Veith, J. C. Neuefeind, R. R. Adzic, P. G. Khalifah, *J. Am. Chem. Soc.* **2014**, DOI: 10.1021/ja4081056.
[23] H. Vrubel, X. Hu, *Angew. Chem.* **2012**, *124*, 12875; *Angew. Chem. Int. Ed.* **2012**, *51*, 12703.
[24] S. Cobo, J. Heidkamp, P.-A. Jacques, J. Fize, V. Fourmond, L. Guetaz, B. Jousselme, V. Ivanova, H. Dau, S. Palacin, M. Fontecave, V. Artero, *Nat. Mater.* **2012**, *11*, 802.
[25] Y. Sun, C. Liu, D. C. Grauer, J. Yano, J. R. Long, P. Yang, C. J. Chang, *J. Am. Chem. Soc.* **2013**, *135*, 17699.
[26] For example: a) V. Artero, M. Chavarot-kerlidou, *Angew. Chem.* **2011**, *123*, 7376; *Angew. Chem. Int. Ed.* **2011**, *50*, 7238; b) M. L. Helm, M. P. Stewart, R. M. Bullock, M. R. DuBois, D. L. DuBois, *Science* **2011**, *333*, 863.
[27] For example: a) E. S. Andreiadis, P.-A. Jacques, P. D. Tran, A. Leyris, M. Chavarot-Kerlidou, B. Jousselme, M. Matheron, J. Pécaut, S. Palacin, M. Fontecave, V. Artero, *Nat. Chem.* **2012**, *5*, 48; b) A. Le Goff, V. Artero, B. Jousselme, P. D. Tran, N. Guillet, R. Métayé, A. Fihri, S. Palacin, M. Fontecave, *Science* **2009**, *326*, 1384.
[28] J. R. McKone, B. F. Sadtler, C. A. Werlang, N. S. Lewis, H. B. Gray, *ACS Catal.* **2013**, *3*, 166.
[29] For example: a) D. Yu, Q. Zhang, L. Dai, *J. Am. Chem. Soc.* **2010**, *132*, 15127; b) D. Deng, L. Yu, X. Chen, G. Wang, L. Jin, X. Pan, J. Deng, G. Sun, X. Bao, *Angew. Chem.* **2013**, *125*, 389; *Angew. Chem. Int. Ed.* **2013**, *52*, 371; c) H. T. Chung, J. H. Won, P. Zelenay, *Nat. Commun.* **2013**, *4*, 1922; d) K. Gong, F. Du, Z. Xia, M. Durstock, L. Dai, *Science* **2009**, *323*, 760.
[30] X. Zou, J. Su, R. Silva, A. Goswami, B. R. Sathe, T. Asefa, *Chem. Commun.* **2013**, *49*, 7522.
[31] For example: a) N. S. Kim, Y. T. Lee, J. Park, J. B. Han, Y. S. Choi, S. Y. Choi, J. Choo, G. H. Lee, *J. Phys. Chem. B* **2003**, *107*, 9249; b) S. Takenaka, M. Ishida, M. Serizawa, E. Tanabe, K. Otsuka, *J. Phys. Chem. B* **2004**, *108*, 11464.
[32] Y. S. Jun, W. H. Hong, M. Antonietti, A. Thomas, *Adv. Mater.* **2009**, *21*, 4270.
[33] G. Wu, K. L. More, C. M. Johnston, P. Zelenay, *Science* **2011**, *332*, 443.